Advances in Military Technology
Vol. 17, No. 2, 2022, pp. 439-455
ISSN 1802-2308, eISSN 2533-4123
DOI 10.3849/aimt.01754

Overlapped Chirp Signals' Parameters Estimation in Radar ESM Station

S. A. Elgamel*

Military Technical College, Cairo, Egypt

The manuscript was received on 29 June 2022 and was accepted after revision for publication as research paper on 25 November 2022.

Abstract:

Three consecutive algorithms are used to estimate the number of multiple overlapped pulsed received chirp signals and their parameters in the electronic support measures (ESM) station noisy receiving window at low signal to noise ratio. The first consecutive algorithm is used to estimate both the number of multiple overlapped received radar signals and the chirp rate of each one in the receiving window. Then, the second consecutive algorithm is used to minimize the additive noise and/or interference in the receiving window by filtering each received chirp signal in the corresponding fractional Fourier domain. The third consecutive algorithm based on WD and Hough transform is used to estimate both the received chirp signal duration and the received chirp signal bandwidth.

Keywords:

fractional Fourier transform, Hough transform, parameters estimation, pulsed received chirp signal, radar ESM, Wigner distribution

1 Introduction

Modern military forces depend heavily on electronic warfare (EW) to produce a complete picture of the electromagnetic battle, such that emitters are detected as soon as they switch on in the operational environment. Detailed parameters and characteristics of these emitters are provided. Radar electronic support measures (ESM) stations are responsible for searching, intercepting, locating, recording, and analyzing radar radiated radio frequency spectrum for the purpose of exploiting such radiations in the support of military operations. Modern radar systems employ low probability of intercept (LPI) signals to avoid the interception by hostile ESM systems. One of the widely used LPI signals is the chirp (linear frequency modulation) signal, which is encoun-

* *Corresponding author: Electronic Warfare Department, Military Technical College, Kobri Elkobba, Cairo, Egypt. Phone: +202-22621908, E-mail: elgamel@mtc.edu.eg. ORCID 0000-0003-0627-5729.*

tered in different radar systems. Thus, ESM stations should develop its detection capabilities by improving their receiving signal processing and analysis. This detailed ESM information is used to control the deployment and operation of electronic counter measures (ECM) stations, since the link between ESM and ECM stations is often automatic. Also, this ESM information is used to ensure effective use of friend chirp radar systems despite the use of enemy ECM.

In [1], Wigner-Ville distribution (WVD) is used as a time frequency (T-F) detection technique and it is combined with Hough-Radon transform (HT) to identify the parameters of radar frequency modulated continuous waveform (FMCW) at low signal to noise ratio (SNR) levels. In [2], WD and HT are used to detect and extract FMCW signals' parameters. A proposed algorithm of Cross-Wigner-Ville and HT (XWHT) is used for detection and parameter extraction of FMCW signals depending on the cross-terms created by WD [2]. The performance of the proposed method is compared with other Wigner-Hough transform-based methods in terms of transform speed, parameter extraction, and detection performance. In [3], a practical approach based on short-time Wigner distribution (STWD) and post processing steps combined with the HT is used for real-time linear FMCW radar signal detection and parameter extraction under low SNR. The proposed algorithms in [3] are applied using an embedded system solution based on field programmable gate arrays with low computational cost. In [4], a combined WD and Choi-William Distribution (CWD) techniques are used for the FMCW signals detection and estimation of its parameters. In [5], analytical formulations, approximations, upper and lower bounds for the angle sweep of maximum magnitude of fractional Fourier transform (FrFT) of mono- and multicomponent LFM signals are presented and a successive coarse-to-fine grid search algorithm to estimate the chirp rates of multicomponent non separable LFM signals is employed. In [6], a proposed method uses the Pseudo-Wigner-Ville Distribution (PWD) as T-F detection technique and HT to identify modulation parameters of FMCW waveforms with −6, −3, 0, 3 and 6 dB SNR levels. In [7], FrFT is used as an asymptotically minimum variance unbiased estimator of the chirp parameters. The chirp rate estimation (using minimum-variance unbiased estimator) is done in one dimensional search space (the fractional Fourier domain (FrFD)) to reduce the computational cost.

From the previous review, the WD is adopted in many signal analysis algorithms to measure the FMCW signal rate and these algorithms suffer from cross terms created by WD. This paper demonstrates overlapped pulsed received chirp signals' parameters estimation in noisy ESM receiving window at low SNR using three consecutive algorithms. The first consecutive algorithm based on FrFT is used to estimate both the number of multiple overlapped received chirp radar signals and the chirp rate of each one in the receiving window as shown in Tab. 1. Then, the second consecutive algorithm based on FrFT filtering is used to minimize the additive noise and/or interference in the receiving window of ESM station by filtering each received chirp signal in the corresponding FrFD. This filtering also minimizes the cross-terms effect appearing due to WD when it is used. The third consecutive algorithm based on WD and Hough transform (HT) is used to estimate the received chirp signal duration and bandwidth. These detailed parameters are used to control the deployment and operation of electronic counter measures (ECM) stations, since the link between ESM and ECM stations is often automatic. Also, the information is used to ensure effective use of friend chirp radar systems despite the use of enemy ECM.

This paper is organized as follows: The mathematical models of FrFT, WD and HT are presented in section 2. Section 3 is intended to explain three consecutive algo-

rithms that are used to estimate the pulsed received chirp signal parameters. In section 4, Matlab simulation and results of the proposed algorithms of overlapped received chirp signals parameters estimation are discussed. Section 5 presents concluding remarks about the work carried out in this paper.

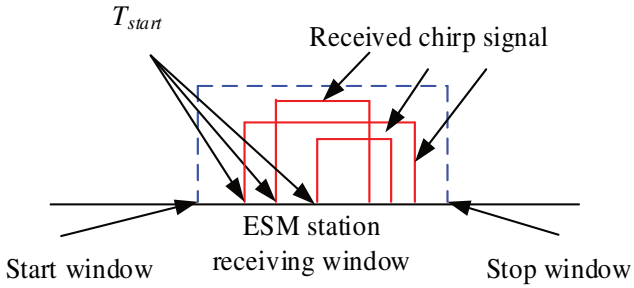

Fig. 1 Radar ESM receiving window

2 FrFT, WD, and HT Mathematical Models

2.1 Fractional Fourier Transform (FrFT)

The FrFT is the generalized formula for the Fourier Transform (FT) that transforms signals into an intermediate domain between time and frequency [8, 9]. The FrFT of order "a" of an arbitrary signal $x(t)$, with an angle θ, is defined as [10]:

$$X_\theta(t_a) = \int_{-\infty}^{\infty} x(t)\, K_\theta(t_a, t)\, \mathrm{d}t \tag{1}$$

where $K_\theta(t_a, t)$ is the FrFT Kernel, t_a is the variable in the a^{th} FrFD, and $\theta = a\pi/2$ with $a \in \mathcal{R}$. $K_\theta(t_a, t)$ is defined as [11].

$$K_\theta(t_a, t) = \begin{cases} \sqrt{\dfrac{1-\mathrm{j}\cot\theta}{2\pi}} \exp\left(\mathrm{j}\dfrac{t^2+t_a^2}{2}\cot\theta - \mathrm{j}t\,t_a\csc\theta\right) & \text{if } \theta \text{ is not a multiple of } \pi \\ \delta(t-t_a) & \text{if } \theta \text{ is a multiple of } 2\pi \\ \delta(t+t_a) & \text{if } \theta+\pi \text{ is a multiple of } 2\pi \end{cases} \tag{2}$$

$X_\theta(t_a)$ is the signal in the intermediate domain between time and frequency, thus it has combined components of the time and frequency. The FrFT is able to process linear chirp signals better than the ordinary FT. A linear chirp signal forms a diagonal line in the T-F plane, and therefore, an order of transformation exists there in which such signals become compact and it appears as a spike. Thus, the optimum FrFT order a_{opt} (or the angle of rotation $\theta_{\text{opt}} = a_{\text{opt}}\pi/2$) transforms the chirp signal to the fractional domain at which this chirp appears as a spike.

The single received chirp signal $x(t)$ may be expressed in the radar ESM receiving window as shown in Fig. 1 in baseband as:

$$x(t)=\begin{cases} A\exp\left(-\mathrm{j}2\pi\varphi_0\right)\exp\left[\mathrm{j}\pi\dfrac{\Delta F}{T}\left(t-T_{\mathrm{start}}-\dfrac{T}{2}\right)^2\right] & T_{\mathrm{start}}<t<T_{\mathrm{start}}+T \\ 0 & \text{anywhere else} \end{cases} \quad (3)$$

where A is the received signal amplitude, φ_0 is the random phase shift, ΔF is the received chirp signal bandwidth, T is the received chirp signal duration, T_{start} is the start time of the received chirp signal in the receiving window.

2.2 Wigner Distribution (WD)

The WD $W_f(t,t_1)$ of a signal x can be defined in terms of the time-domain representation $x(t)$ of that signal as [11]

$$W_f\left(t,t_1\right)=\int_{-\infty}^{\infty} x\left(t+t'/2\right)x^*\left(t-t'/2\right)\exp\left(-\mathrm{j}2\pi t_1 t'\right)\mathrm{d}t' \quad (4)$$

where t_1 is the special case of t_a at $a = 1$ and $x^*(t)$ is the complex conjugate of $x(t)$.

It is shown that the WD of $f^a(t)$ is merely a rotation version of the WD of $x(t)$ as [11]

$$W_{f_a}\left(t,t_1\right)=W_f\left(t\cos\theta-t_1\sin\theta,t\sin\theta+t_1\cos\theta\right) \quad (5)$$

Thus, the WD of a signal and its FrFT are related by a rotation over an angle θ. In other words, rotation of WD of a signal (ellipse shape) with angle θ (shown in Fig. 2a) results in a WD of this signal in the FrFD as illustrated Fig. 2b [11].

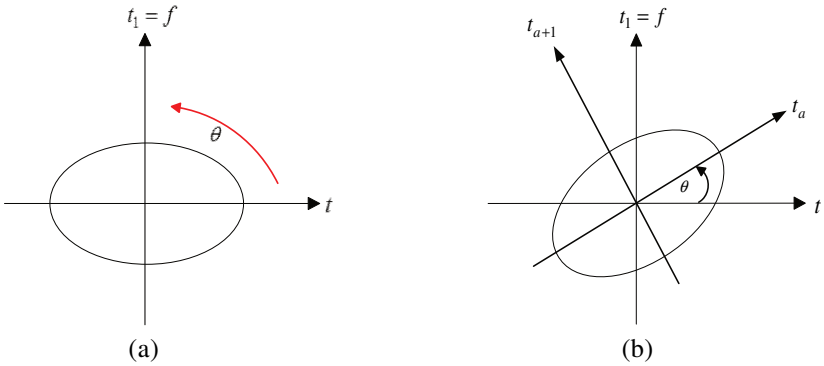

Fig. 2 WD of a signal in different domains

2.3 Hough Transform (HT)

The Hough transform (HT) is designed to detect lines in an image, using the parametric representation of a line [12],

$$\rho = x\cos\phi + y\cos\phi \quad (6)$$

where ρ is the distance from the origin to the line along a vector perpendicular to the line, ϕ is the angle between the x-axis and this vector. The HT is used to generate a parameter space matrix whose rows and columns correspond to these ρ and ϕ values, respectively. Once the HT is applied to an input image, the peak values in the parameter space are then determined. These peak values represent potential line segments in

the input image. In turn, the end points of those line segments are obtained. Finally, small gaps in such lines are filled automatically.

3 Parameters' Estimation of Overlapped Pulsed Chirp Signals

Three consecutive algorithms are applied to estimate the received chirp signal parameters at low SNR. These algorithms are: FrFT of a received chirp signal with different transformation angle algorithm, filtering the received signal based on FrFT algorithm, WD and HT image processing algorithm as shown in Fig. 3. In the next sub-sections, the three algorithms will be discussed in details.

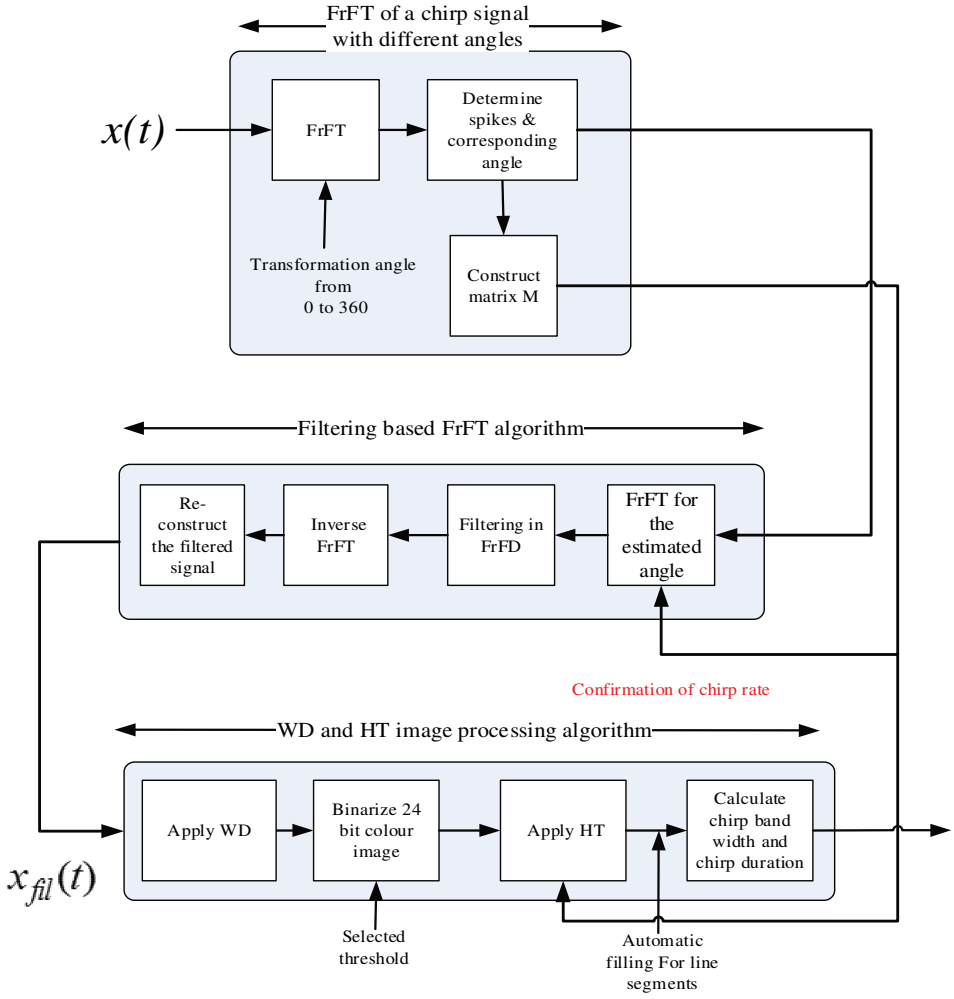

Fig. 3 Functional block diagram of chirp parameters estimation

3.1 FrFT of a Chirp Signal with Different Transformation Angle Algorithm

The linear chirp signal appears as a spike in its optimal FrFD because this domain is perpendicular to the line representing the chirp signal in the T-F domain. Thus, transforming the received signal (in the ESM receiving window) to all angles from 0° to 360° results in the appearance of a number of spikes. The number of these spikes is equal to the number of the received chirp signals even if the receiving window suffers from the added noise and/or intended interference signal. The angle at which the received chirp signal appears as a spike is the optimal FrFD angle, thus the chirp rate (slope) of this chirp signal is perpendicular to it FrFD. The proposed algorithm is used to build the matrix $\boldsymbol{M}$ with $m \times n$ dimension as shown in Algorithm 1. The row dimension m represents the fractional samples in the a^{th} FrFD while the column dimension n represents the transformation parameter "a" from 0 to 2 (which is corresponding to the angles θ from 0° to 360°) as:

$$\boldsymbol{M} = \left[X_\theta\left(t_{a_1}\right) X_\theta\left(t_{a_2}\right)\ X_\theta\left(t_{a_3}\right) ... X_\theta\left(t_{\mathrm{a}_n}\right) \right]^{\mathrm{T}} \tag{7}$$

The FrFT of a chirp signal with different transformation parameter "a" algorithm is shown in Algorithm 1. In the proposed sub-algorithm, if the received signal $x(t)$ is transformed to $X_\theta(t_a)$in all FrFD corresponding to all angles θ (from 0° to 360°) using (1), then the number of spikes is counted and its corresponding angles are determined. The number of spikes is equal to the number of overlapped linear chirp signals in the receiving window while the corresponding angles determine the FrFD which is perpendicular to the chirp signal rates. Each transformed signal $X_\theta(t_a)$ is normalized with respect to its maximum and then it is used as a new row to construct matrix $\boldsymbol{M}$ $(m \times n)$ dimension with the new transformation parameters "a". The matrix $\boldsymbol{M}$ is plotted to show the received signal in the FrFD corresponding to a transformation angle from 0° to 360° to **confirm** the results obtained in step **3** in the algorithm. This is done in such a way that the number of spikes equals the number of narrowest bottleneck white points (in the plotting of matrix $\boldsymbol{M}$). The corresponding fractional order "a" of each bottleneck is determined, thus the corresponding angle θ_{opt} is calculated.

3.2 Filtering the Received Signal Based on FrFT Algorithm

The received signal in the receiving window of ESM station suffers from the additive noise and/or intended interference signal. Thus, a proposed filtering algorithm based on FrFT as shown in Algorithm 2, is used to minimize these interferences and consequently to minimize the cross-terms effect due to WD, if it is used to estimate chirp signal parameters. In Algorithm 2, according to the estimated number of overlapped chirp signal K and the estimate chirp rate angles (outputs from the Algorithm 1), the filtering algorithm is repeated K times. For the K times, the received signal $x(t)$ is transformed to $X_\theta(t_a)$ in all FrFD corresponding to K estimated angles θ_{opt}. FrFD filtering is done by keeping the spike sample magnitude and its adjacent samples magnitude. Then, all other fractional samples magnitude in the receiving windows are forced to be zero. Thus, the filtering process keeps only one chirp signal and removes all other chirp signals, as well as the additive interference. Applying inverse FrFT, the filtered signal FrFD returns back to time domain. The previous FrFD filtering process is repeated K times (according to the estimated number of overlapped chirp signal). Then, the K^{th} filtered signal is added to each other to reconstruct $x_{\text{fil}}(t)$.

Algorithm 1: FrFT of a chirp signal with different transformation parameter "a"

Given:

The received signal $x(t)$ in the ESM station receiving window

Required:

Construct and plot the matrix $\boldsymbol{M}$ ($m \times n$ dimension)

The number of spikes K represents (the number of overlapped chirp signals)

The corresponding a for each spike

Initialize:

$a = 0$

1 For $0 \le a \le 2$ **do** step (responsible for the dimension n in matrix $\boldsymbol{M}$)

2 Do FrFT of $x(t)$ using Eq.1 as $X_\theta(t_a) = \mathrm{FrFT}[x(t),a]$

3 Count the number of spike K (if it exists) and determine corresponding angle $\theta_{\mathrm{opt}} = a_{\mathrm{opt}}\pi/2$

4 Normalize $X_\theta(t_a)$ as $X_\theta(t_a)_N = \dfrac{\mathrm{abs}\left[X_\theta(t_a)\right]}{\max\left[X_\theta(t_a)\right]}$ m dimension in matrix $\boldsymbol{M}$

5 $X_\theta(t_a)_N$ be new row in matrix $\boldsymbol{M}$

6 End For

7 Plot the matrix $\boldsymbol{M}$

Algorithm 2: Filtering the received signal based on FrFT

Given:

The matrix $\boldsymbol{M}$ ($m \times n$ dimension)

The number of spikes K

The corresponding a for each spike and the corresponding estimated angle θ_{opt}

The received signal $x(t)$

Required:

Filtering the received signal $x(t)$ in the k^{th} FrFD before returning back to time domain $x_{\mathrm{fil}}(t)$

1 For $1 \le k \le K$ **do**

2 Do FrFT of $x(t)$ using Eq. (1) as $X_\theta(t_a) = \mathrm{FrFT}\left[x(t), a\right]$ to transform the received signal $x(t)$ to the k^{th} FrFD according to the estimated angle θ_{opt}

3 Filtering in the FrFD

4 Apply inverse FrFT by applying Eq. 1 as $x(t) = \mathrm{FrFT}\left[X_\theta(t_a), -a\right]$

5 Sum the K^{th} filtered signal again in the time domain to reconstruct the filtered received signal $x_{\mathrm{fil}}(t)$

6 End For

3.3 WD and HT Image Processing Algorithm

The filtered received signal $x_{fil}(t)$ (output of the Algorithm 2) passes through Algorithm 3. $x_{fil}(t)$ is applied to WD process in Eq. (4). WD output is a matrix with $m' \times n'$ dimension in T-F plane, from which the lines that correspond to the chirp signals have to be identified. One approach is to consider the $m' \times n'$ matrix as an image. To identify such lines in that image, it has to be binarized first (i.e., converted into the black & white color space). Then, the standard HT in Eq. (5) is applied to the resultant image as a line detector, yielding a set of detected line segments. Finally, the starting point, the ending point, as well as the line slope are determined for all detected lines. Each line points coordinates are used to determine the chirp signal bandwidth and chirp duration using the difference in samples in x axis and the difference in samples in y axis, then mapping these differences to time and frequency, respectively.

Algorithm 3: WD and HT image processing

Given:

The confirmed number of spikes K and the corresponding estimated angle θ_{opt}

The filtered received signal $x_{fil}(t)$

Required:

Estimation of pulsed chirp signal parameters (chirp rate, chirp bandwidth, and chirp duration)

1 Apply WD to the filtered received signal $x_{fil}(t)$
2 The output 24 bit color image is binarized by a selected threshold to be black and white image.
3 Apply HT to detect lines in the black and white image; these lines appear as segments. The lines (if exist) due to WD cross terms are neglected (only the confirmed chirp rates are considered).
4 Small gaps in the line segments are filled automatically.
5 Estimation of chirp signal parameters (chirp rate, chirp bandwidth, and chirp duration).

4 Chirp Signals Parameters' Simulation and Estimation of Results

Three simulated chirp signals with the parameters shown in Tab. 1 are considered to fall in the receiving window for an ESM station. The parameters are chosen to demonstrate the idea with challenge of overlapping in time and frequency.

Tab. 1 Parameters of simulated overlapped chirp signals

Signal No.	Amplitude	Start time [s]	Chirp duration [s]	Start frequency [Hz]	Stop frequency [Hz]	Chirp bandwidth [Hz]
1	1.2	0.5	2.5	50	250	200
2	1.1	1.5	2.0	100	220	120
3	1.3	2.5	1.0	20	200	180

4.1 Simulation of the Overlapped Received Chirp Signals in the ESM Station

The receiving window of ESM station is considered to be 5 s. The start time of each chirp signal is the time at which the received signal starts in the receiving window as demonstrated in Fig. 1. The start frequency, the stop frequency, and the chirp duration are the simulated received chirp signal parameters using Eq. (3). Thus, the proposed algorithms in the ESM processor are applied to estimate these parameters as in Fig. 3. The receiving window is considered to be corrupted with added noise (or inference), such as SNR = −3 dB. Fig. 4 demonstrates three chirp signals number 1, 2, and 3, (in the time domain) with different amplitudes using the parameters in Tab. 1. Figs 4a 4b and 4c show the chirp signals number 1, 2, and 3 respectively. Fig. 4d shows the ESM receiving window with the sum of these three chirp signals without any additive noise. Fig. 4e demonstrates the problem of applying WD only using Eq. (4); it is clear that cross terms appear especially in the region between the overlapped chirp signals and sometimes they appear as chirp-like signals. In Fig. 4f, the receiving window is corrupted with added noise, with SNR = −3 dB. Fig. 4g shows applying WD for the noisy overlapped chirp signals and it is clear that it is hard to distinguish between chirp signals and cross terms components.

4.2 Simulation of ESM Received Signal Using FrFT with Different Transformation Angle Algorithm

Applying the proposed Algorithm 1 for the simulated received signal (in the receiving window in the ESM station) shown in Fig. 4f, the signal is transformed to the fractional domains corresponding to all angles from 0° to 360° with transformation order "a" and a step equal to 0.001. Three spikes appear at three fractional orders 1.242, 1.185, and 1.466 due to the three received chirp signals 1, 2, and 3 as shown in Figs 5a, 5b and 5c, respectively. Thus, the corresponding estimated FrFD angles are 111.78°, 106.65°, and 131.94° determined for the fractional order 1.242, 1.185, and 1.466, respectively. A normalized $\boldsymbol{M}$ matrix with $5\,000 \times 2\,000$ is constructed and plotted as shown in Fig. 5d. In Fig. 5d, three bottlenecks appear at fractional order 1.242, 1.185, and 1.466 are used to confirm the results obtained before. The estimated FrFD angles and the corresponding chirp rates are shown in Tab. 2. Applying the proposed Algorithm 1 hundred times, it has been found that the higher SNR, the higher ability to determine the number of overlapped chirp signals and their corresponding estimated FrFD angles. Algorithm 1 achieves adequate estimation for the number of overlapped chirp signals and their corresponding estimated FrFD angles at SNR as low as −12 dB.

Tab. 2 Estimation of chirp rates

Signal No.	Estimated fractional order	Estimated FrFD angle	Estimated chirp rate
1	1.242	111.78	21.78
2	1.185	106.65	16.65
3	1.466	131.94	41.94

DOI 10.3849/aimt.01754

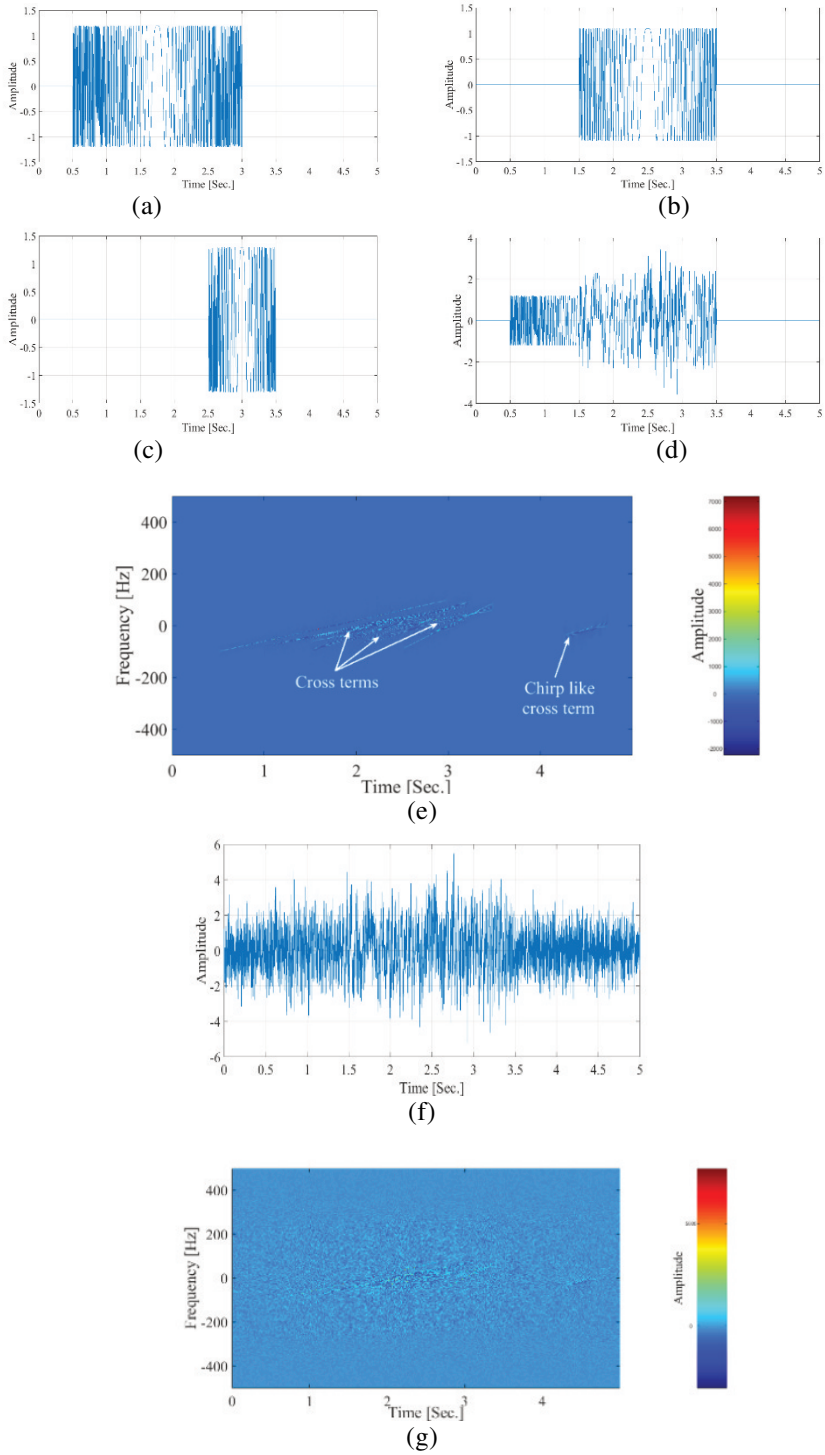

Fig. 4 Simulation of chirp signals in ESM receiving window

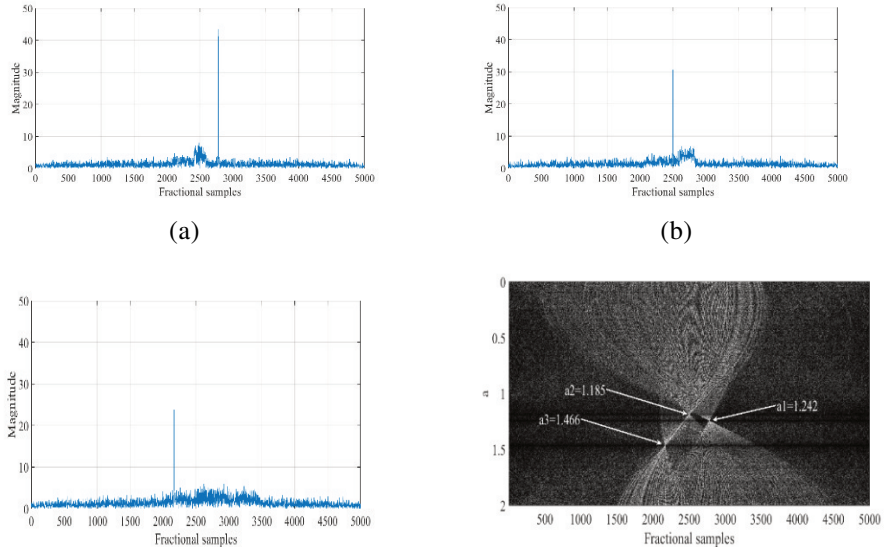

Fig. 5 Transformation of the signal in ESM receiving window in different FrFD

4.3 Simulation of Filtering the Received Signal Based on FrFT Algorithm

The proposed filtering algorithm based on FrFT shown in Algorithm 2 is repeated three times according to the results from Algorithm 1. Thus, the received signal is transformed to the three fractional domains 1.242, 1.185, and 1.466 corresponding to the estimated angles in Tab. 2. Each time, filtering is performed by keeping the spike sample magnitude (at 2 779, 2 500, 2 166 respectively) and its adjacent samples magnitude (five samples to the right and five samples to the left), and by forcing the rest samples magnitude to be equal to zero as shown in Figs 6a, 6b and 6c, for the three fractional angles, respectively. The sum of the filtered received signal after applying inverse FrFT (in the time domain) using the fractional orders −1.242, −1.185, and −1.466 is shown in Fig. 6d. Thus, the effect of filtering the added noise is clear comparing with non-noisy overlapped chirp signal and noisy overlapped chirp in Figs 4d and 4f, respectively. In Fig. 6e, the final reconstructed filtered simulated received signal $x_{\text{fil}}(t)$ in different FrFD, Fig. 6e gives more accurate results comparing with Fig. 5d.

4.4 Simulation of WD and HT Image Processing Algorithm

The simulated filtered received signal $x_{\text{fil}}(t)$ yield from Algorithm 2 is applied to the third algorithm in Algorithm 3. The WD output appears as three dotted lines due to the three chirp signals in the T-F domain and some dotted lines appear as other chirp like signals, but it is due to cross-terms created by WD as shown in Fig. 7a. The image in Fig. 7a is cast in 24-bit color format using threshold as shown in Fig. 7b. Having the HT applied to that black and white image, a number of lines appears in the colored image as separated segments. In turn, such gaps between segments can be filled automatically as shown in Fig. 6c forming "complete" lines. The line segments, with confirmed chirp rate, are only considered. Then, the coordinates of end points of the "complete" lines are

determined. The samples difference in the x-axis is mapped to time and it represents the chirp duration while the samples difference in y-axis is mapped to frequency and it represents the chirp bandwidth. The average estimation of parameters of the simulated overlapped chirp signals at SNR = −3dB is shown in Tab. 3. Comparing the estimated parameters in Tab. 3 with the original simulated radar parameters in Tab. 1, it has been found that the proposed three consecutive algorithms succeed in estimating: there are three chirp signals only (neglect the chirp like cross terms). Also, the proposed three consecutive algorithms estimate the three signal parameters introduced in Tab. 1 with adequate error.

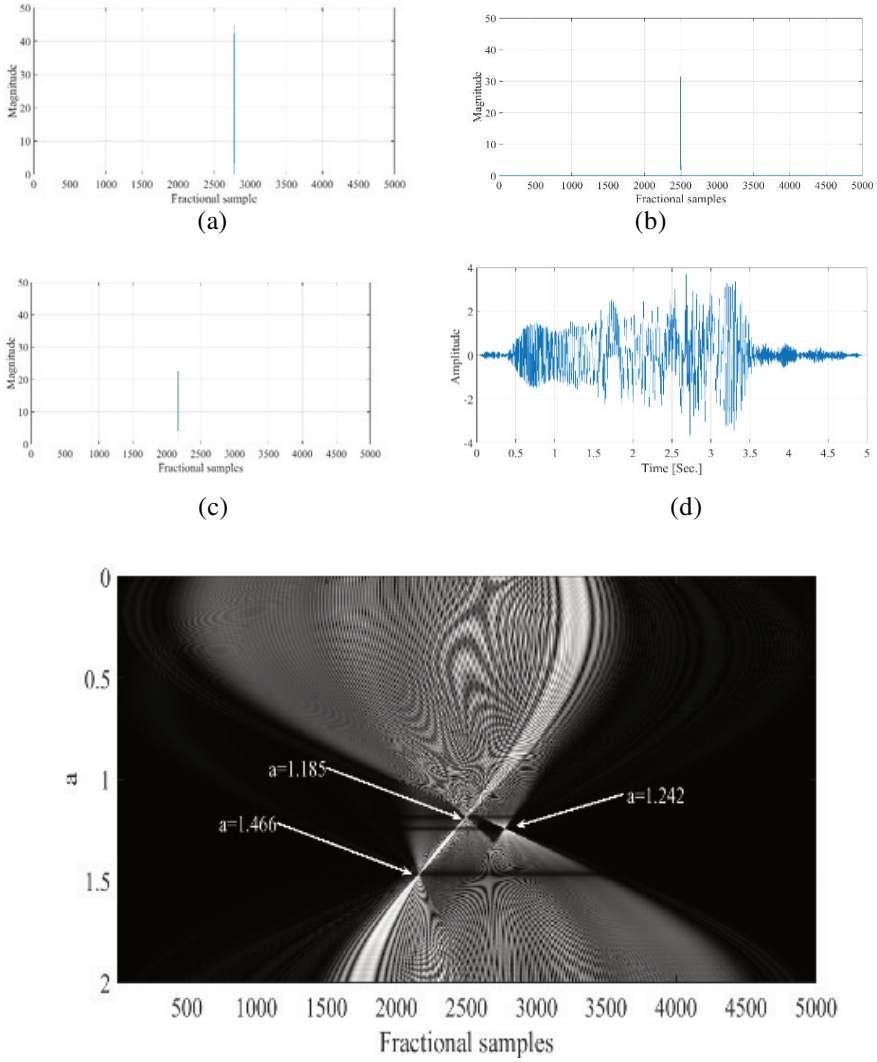

Fig. 6 Filtering the received signal in different FrFD

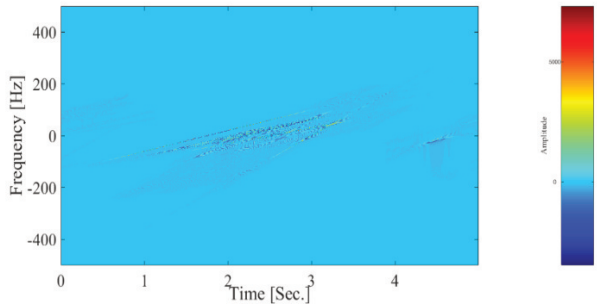

(a)

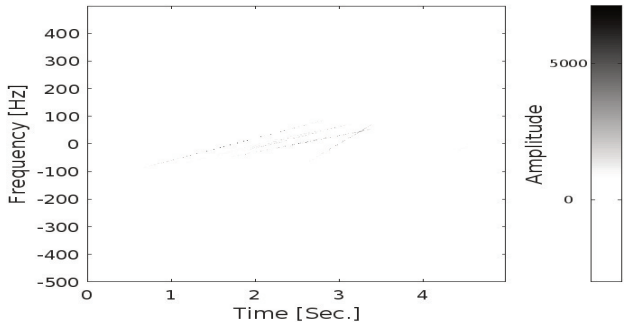

(b)

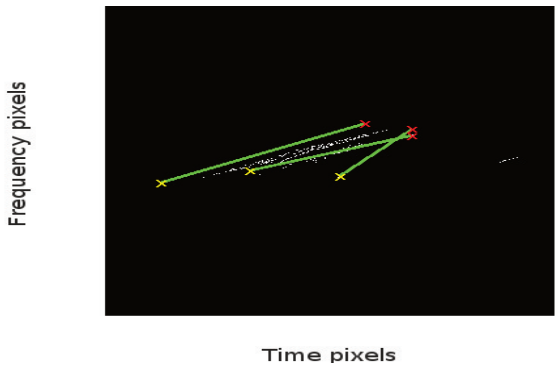

(c)

Fig. 7 Simulation of WD and HT algorithms

Tab. 3 Average estimation parameters of simulated overlapped chirp signals

Signal No.	Estimated chirp angle [degree]	Estimated chirp rate	Average estimated chirp duration [s]	Average estimated chirp bandwidth [Hz]
1	21.08	0.39	2.481	198.52
2	16.69	0.30	1.951	120.61
3	41.98	0.90	0.933	167.05

4.5 Performance Evaluation of the Proposed Algorithms

a. Simulated chirp signals at different SNR

The root mean square error (RMSE) percentage for the estimated parameters (chirp rate, chirp duration, and chirp bandwidth) for the three chirp signals at different SNR is shown in Tab. 4. It could be noticed from Tab. 4 that the added noise hardly affects the estimation of start point and end point coordinates of each line (represent a chirp signal in T-F domain); thus, the chirp duration and chirp bandwidth are hardly affected. But, the estimation of each line slope that corresponds to chirp rate is less affected by the added noise. It is illustrated in Tab. 4 that the RMSE percentage for simulated overlapped chirp signals parameters increase when the SNR decrease.

Tab. 4 RMSE of the estimation parameters of simulated overlapped chirp signals

Signal No.	RMSE at SNR = −5 dB [%]			RMSE at SNR = −8 dB [%]			RMSE at SNR = −10 dB [%]		
	Chirp rate	Chirp duration	Chirp bandwidth	Chirp rate	Chirp duration	Chirp bandwidth	Chirp rate	Chirp duration	Chirp bandwidth
1	0.05	7.56	7.52	0.055	8.56	8.56	0.057	10.56	10.52
2	0.06	9.47	9.98	0.067	10.47	10.63	0.068	11.47	11.98
3	0.05	10.21	10.35	0.056	11.21	11.75	0.067	12.54	12.36

b. Real chirp signals in high power interference scenario

DARPA/Navy Mountaintop Program emulate a real airborne monopulse tracking radar (chirp radars) [13; 14]. A radar-jammer parameters are shown in Tab. 5 (considering the Mountaintop Program jamming scenario). The real jamming data is an experimental dataset "File stap3001". It was collected as part of the DARPA/Navy Mountaintop Program. The real jamming radar data "File stap3001" is pseudo-random signal noise and at an azimuth of 302° relative to true North. Therefore the jammer is at angle 42° from the radar look direction so the interference enters the radar through the side lobe [13-15]. Thus for this high power jamming scenario, the considered received signal-to-interference noise ratio (SINR) is approximately equal to −8 dB [16]. To apply the proposed consecutive algorithms in real scenario, consider the ESM station replaces the radar system and the receiving window is the same as the receiving window of the radar system as in Tab. 5. Another simulated chirp radar signal is generated and it is injected to the ESM receiving window with the radar parameters in Tab. 6. The proposed consecutive algorithms are applied to the received signal in ESM receiving window from the two targets according to radar-jammer scenario parameters, as shown in Tabs 5 and 6. The results from consecutive algorithms (following all steps illustrated in Algorithms 1, 2, and 3) show that there are two chirp signals in the receiving ESM window (cancel the cross-terms effect appears due to WD). The RMSE percentage for the estimated parameters (chirp rate, chirp duration, and chirp bandwidth) for the two target signals (two chirp signals) at SINR = −8 dB is shown in Tab. 7. Comparing the RMSE results in Tabs 4 and 7 at the same SINR = −8 dB, it could be noticed that the results in Tab. 7 are better than those in Tab. 4. The lower RMSE in Tab. 7 rather than in Tab. 4 is caused by hard challenge of overlapping in time and frequency in the considered simulation situation.

Tab. 5 Parameters of radar-jamming scenario

No.	Parameters	Value
Radar parameters		
1	Radar antenna elements	ULA 14
2	Antenna spacing	1/3 m
3	Chirp pulse width	500 kHz
4	Carrier frequency	435 MHz
5	Baseband sampling frequency	10 MHz
6	Radar operating range	100:200 bins
7	Starting window	865 μs
8	Window duration	403 μs
9	Pulse repletion interval	1.6 ms
10	Pulse duration	100 μs
Target parameters		
1	Target range bin	150
2	Target angle (from the look direction)	32°
3	Target SNR	56 dB
Jammer parameters		
1	Jamming type	Direct-path barrage noise jammer (pseudo-random signal noise)
2	Jamming direction	42°
3	Noise jamming bandwidth	600 kHz
4	Jammer range from the radar	65 km

Tab. 6 Simulated received radar signal in the ESM station receiving window

No.	Parameters	Value
ESM parameters		
1	Baseband sampling frequency	10 MHz
2	ESM operating range	100:200 bins
3	ESM Starting window	865 μs
4	ESM Window duration	403 μs
Simulated injected target parameters		
1	Chirp pulse width	550 KHz
2	Target range bin	160
3	Target SNR	56 dB
4	Pulse repletion interval	1.2 ms
5	Pulse duration	80 μs

Tab. 7 RMSE of the estimation parameters of real chirp signals

Target No.	Parameters RMSE [%] at SINR = −8 dB		
	Chirp rate	Chirp duration	Chirp bandwidth
1	0.066	8.66	8.76
2	0.054	8.97	8.82

5 Conclusion

This paper discusses proposed three consecutive algorithms to estimate the number of overlapped chirp signals and the chirp signal parameters (chirp rates, chirp duration, and chirp bandwidth) at lower SNR in the ESM station receiving window. These algorithms used in the ESM processor are: FrFT of a chirp signal with different transformation angle algorithm, filtering the received signal based on FrFT algorithm, WD and HT image processing algorithm, respectively. The first algorithm is used to estimate the number of overlapped chirp signals and the corresponding chirp signal rates by transforming the received signal in receiving window to all possible FrFD and to count the number of spikes and the corresponding angle fractional domain. The second algorithm is used to filter the signal in receiving window from additive noise and/or interference. This is done by transforming it to the fractional domains corresponding to the estimated angles results from the first algorithm. The filtering is done by keeping the spike sample and its adjacent samples and returning back to the time domain. The third algorithm is used to estimate and confirm the number and the chirp rates by applying WD. Only the estimated ones in the first algorithm are considered. Using HT, the chirp signals are determined by lines and using image processing to determine the lines starting points and ending points coordinates. The difference in the *x*-axis is mapped to time [s] and it represents chirp duration while the difference in *y*-axis is mapped frequency [Hz] and it represents the chirp bandwidth. RMSE percentage is used to measure the estimation of chirp parameters at different SNR. RMSE percentage for simulated overlapped chirp signals parameters increase when the SNR decrease, it reached 0.068 %, 12.54 %, and 12.36 % for estimating the chirp rate, chirp duration, chirp bandwidth respectively at SNR = −10 dB. The proposed consecutive algorithms achieved adequate estimation chirp parameters at SNR as low as −12 dB. The proposed consecutive algorithms are also applied to real radar-jammer scenarios at SINR = −8 dB and get adequate RMSE for chirp parameters estimation.

References

[1] GULUM, T.O., A.Y. ERDOGAN, T. YILDIRIM and P.E. PACE. A Parameter Extraction Technique for FMCW Radar Signals Using Wigner-Hough-Radon Transform. In: *Proceedings of the 2012 IEEE Radar Conference*. Atlanta: IEEE, 2012, pp. 0847-0852. DOI 10.1109/RADAR.2012.6212255.

[2] ERDOGAN, A.Y., T.O. GULUM, L. DURAK-ATA, T. YILDIRIM and P.E. PACE. FMCW Signal Detection and Parameter Extraction by Cross Wigner-Hough Transform. *IEEE Transactions on Aerospace and Electronic Systems,* 2017, **53**(1), pp. 334-344. DOI 10.1109/TAES.2017.2650518.

[3] GUNER, K.K., T.O. GULUM and B. ERKMEN. FPGA-Based Wigner-Hough Transform System for Detection and Parameter Extraction of LPI Radar LFMCW

Signals. *IEEE Transactions on Instrumentation and Measurement*, 2021, **70**, 2003515. DOI 10.1109/TIM.2021.3060584.

[4] HOSSEINI, S.M. and R. MOHSENI. Interception FMCW Radar Using Wigner-Ville Distribution (WVD). *Majlesi Journal of Telecommunication Devices*, 2013, **2**(4), pp. 153-159. ISSN 2423-4117.

[5] SERBES, A. On the Estimation of LFM Signal Parameters: Analytical Formulation. *IEEE Transactions on Aerospace and Electronic Systems*, 2018, **54**(2), pp. 848-860. DOI 10.1109/TAES.2017.2767978.

[6] GULUM, T.O., A.Y. ERDOGAN, T. YILDIRIM and L.D. ATA. Parameter Extraction of FMCW Modulated Radar Signals Using Wigner-Hough Transform. In: *Proceedings of the 2011 IEEE 12th International Symposium on Computational Intelligence and Informatics (CINTI)*. Budapest: IEEE, 2011, pp. 465-468. DOI 10.1109/CINTI.2011.6108551.

[7] ALDIMASHKI, O. and A. SERBES. Performance of Chirp Parameter Estimation in the Fractional Fourier Domains and an Algorithm for Fast Chirp-Rate Estimation. *IEEE Transactions on Aerospace and Electronic Systems*, 2020, **56**(5), pp. 3685-3700. DOI 10.1109/TAES.2020.2981268.

[8] KUTAY, M.A., H.M. OZAKTAS, O. ANKAN and L. ONURAL. Optimal Filtering in Fractional Fourier Domains. *IEEE Transactions on Signal Processing*, 1997, **45**(5), pp. 1129-1143. DOI 10.1109/78.575688.

[9] KUTAY, M.A., H.M. OZAKTAS, L. ONURAL and O. ARIKAN. Optimal Filtering in Fractional Fourier Domains. In: *1995 International Conference on Acoustics, Speech, and Signal Processing*. Detroit: IEEE, 1995. DOI 10.1109/ICASSP.1995.480329.

[10] CANDAN, C., M.A. KUTAY and H.M. OZAKTAS. The Discrete Fractional Fourier Transform. *IEEE Transactions on Signal Processing*, 2000, **48**(5), 1329-1337. DOI 10.1109/78.839980.

[11] OZAKTAS, H.M., O. ARIKAN, M.A. KUTAY and G. BOZDAGI. Digital Computation of the Fractional Fourier Transform. *IEEE Transactions on Signal Processing*, 1996, **44**(9), 2141-2150. DOI 10.1109/78.536672.

[12] GONZALES, R.C. and R.E. WOODS. *Digital Image Processing*. 4th ed. Bengaluru: Pearson India, 2018. ISBN 978-0-13-335672-8.

[13] TITI, G.W. and D.F. MARSHALL. The ARPA/NAVY Mountaintop Program: Adaptive Signal Processing for Airborne Early Warning Radar. In: *1996 IEEE International Conference on Acoustics, Speech, and Signal Processing Conference Proceedings*. Atlanta: IEEE, 1996, pp. 1165-1168. DOI 10.1109/ICASSP.1996.543572.

[14] Mountain Top Radar [online]. [viewed 2022-04-02]. Available from: http://spib.linse.ufsc.br/radar.html#:~:text=The%20Mountaintop%20Program%20is%20an,obtained%20from%20MIT%20Lincoln%20Laboratory

[15] JOHNSON, D.H. and D.E. DUDGEON. *Array Signal Processing: Concepts and Techniques*. London: Pearson, 1993. ISBN 978-0-13-048513-6.

[16] ELGAMEL, S.A. and J.J. SORAGHAN. Using EMD-FrFT Filtering to Mitigate Very High Power Interference in Chirp Tracking Radars. *IEEE Signal Processing Letters*, 2011, **18**(4), pp. 263-266. DOI 10.1109/LSP.2011.2115239.